

Characterization of Printed Reflectarray Elements on Variable Substrate Thicknesses

M. Y. Ismail, Arslan Kiyani

Abstract—Narrow bandwidth and high loss performance limits the use of reflectarray antennas in some applications. This article reports on the feasibility of employing strategic reflectarray resonant elements to characterize the reflectivity performance of reflectarrays in X-band frequency range. Strategic reflectarray resonant elements incorporating variable substrate thicknesses ranging from 0.016λ to 0.052λ have been analyzed in terms of reflection loss and reflection phase performance. The effect of substrate thickness has been validated by using waveguide scattering parameter technique. It has been demonstrated that as the substrate thickness is increased from 0.508mm to 1.57mm the measured reflection loss of dipole element decreased from 5.66dB to 3.70dB with increment in 10% bandwidth of 39MHz to 64MHz. Similarly the measured reflection loss of triangular loop element is decreased from 20.25dB to 7.02dB with an increment in 10% bandwidth of 12MHz to 23MHz. The results also show a significant decrease in the slope of reflection phase curve as well. A Figure of Merit (FoM) has also been defined for the comparison of static phase range of resonant elements under consideration. Moreover, a novel numerical model based on analytical equations has been established incorporating the material properties of dielectric substrate and electrical properties of different reflectarray resonant elements to obtain the progressive phase distribution for each individual reflectarray resonant element.

Keywords—Numerical model, Reflectarray resonant elements, Scattering parameter measurements, Variable substrate thickness.

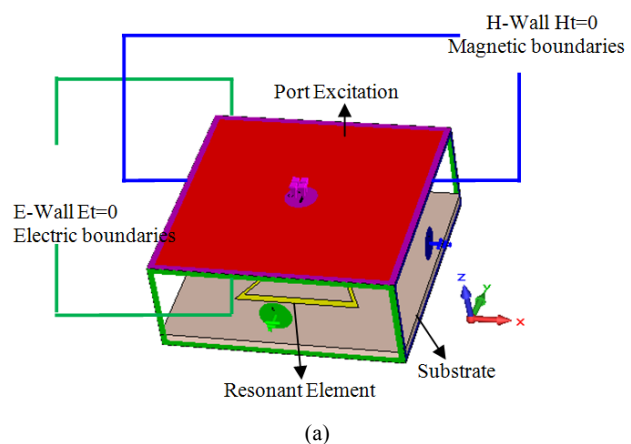
I. INTRODUCTION

REFLECTARRAYS are proposed as the best alternative to mitigate the various disadvantages of bulky parabolic reflectors and expensive phased arrays [1]. The need for finding an alternative arises due to some of the limitations associated with the conventional structures. For example the use of parabolic reflectors is limited particularly at higher microwave frequencies [2], due to the curvature of reflector resulting in an increased weight and size of the antenna. Moreover it is difficult to achieve the wide-angle electronic beam scanning. However high gain array antennas utilize the controllable phase shifters making them feasible of wide-angle beam scanning as compared to the parabolic reflectors. They also require high cost amplifier modules which make them a very expensive solution for various high gain applications [2]. On the other hand flat structure, low cost and easy deploy ability of reflectarrays projected them as a promising candidate for future high gain applications.

A Microstrip reflectarray consists of an array of resonant

elements printed on top of dielectric substrate backed by a ground plane [3]. A feed antenna is placed at a particular distance to illuminate the array, whose individual elements scatter the incident field with proper phase distribution required to make a planar wave in front of the aperture of reflectarray [3], [4]. Various approaches have been proposed in the past for the progressive phase distribution of the reflectarrays such as, square patches of variable size [5], [6], identical patches of variable-length stub [7], identical planar elements of variable rotation [8], cross dipoles [9], [10], ring elements [11], [12] and the liquid crystal based reflectarray antennas [13] to vary the effect of different path length. Despite number of advantages the bandwidth and reflection loss performance are considered as the main shortcomings of reflectarrays [14], [15]. The bandwidth is limited mainly due to the narrow bandwidth of the resonant elements and differential spatial phase delay due to the extended path length between the feed and reflectarray [16]. The feed antenna bandwidth and array element spacing are also among the factors responsible for limited bandwidth performance, but they are not of serious concern if the bandwidth requirement is less than 15% [3]. Many researchers have been working on various possible techniques to increase the bandwidth and up to 15% bandwidth has been reported in [17].

In this work the effect of using variable substrate thickness on the performance characterization of reflectarrays has been demonstrated. The practical validation of predicted results obtained from commercially available CST computer model based has been carried out using waveguide simulator technique. A mathematical model has also been developed for progressive phase distribution of various reflectarray resonant elements.



M. Y. Ismail and Arslan Kiyani are with the Wireless and Radio Science Centre (WARAS), Universiti Tun Hussein Onn Malaysia (UTHM), Batu Pahat, 86400, Johor, Malaysia (e-mail: yusofi@uthm.edu.my, arslan.kiyani@gmail.com).

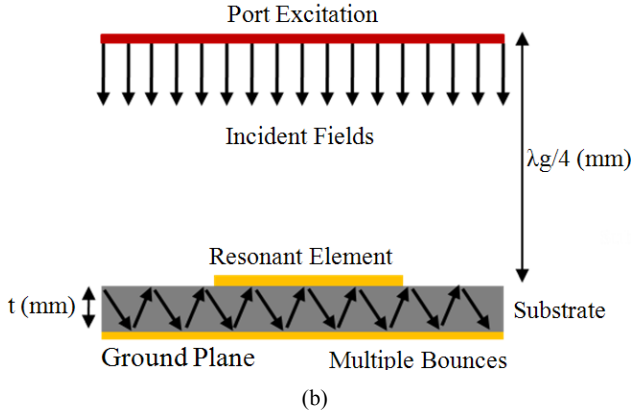


Fig. 1 (a) Built model of reflectarray unit cell (b) Dielectric absorption in reflectarrays

II. THEORETICAL ANALYSIS

A. Reflectarray Losses

Reflectarrays attribute dielectric loss due to the dielectric absorption in the substrate and conductor losses due to the conductivity of the conducting material utilized for the design of reflectarray resonant elements [4], [18]. Thus the reflection loss performance of the reflectarrays depends on the material properties and thickness of the dielectric substrate. The reflection loss can be given as (1).

$$R_L = \alpha_d + \alpha_c \quad (1)$$

where, R_L is the reflection loss and α_d and α_c are the attenuation due to the dielectric substrate and conductor loss respectively which can be calculated using (2) and (3) as:

$$\alpha_d = \frac{\omega}{2} \sqrt{(\mu_o \epsilon_o \epsilon_r)} \tan \delta \quad (2)$$

$$\alpha_c = \frac{8.68}{WZ_m} \sqrt{\frac{\omega \mu_o}{2\sigma_c}} (db/cm) \quad (3)$$

A unit cell reflectarray element with proper boundary conditions is shown in Fig. 1 (a). Fig. 1 (a) shows that the incident electric fields create E-walls (top and bottom walls) and H-walls (side walls) around the resonating structure. Moreover, the dielectric absorption into the substrate region of reflectarray antenna is depicted in Fig. 1. It can be seen that the port excitation is placed at a distance of $\lambda_g/4$ to incident the electric fields on the reflectarray resonant element and the dielectric substrate (t). These incident fields are being absorbed by the substrate region resulting in multiple bounces phenomenon. Thus the intensity of dielectric absorption in a particular substrate determines the reflection loss performance which can be seen from Fig. 1 (b). For thinner substrates, a number of rapid multiple bounces will occur due to higher dielectric absorption which contributes the higher reflection loss performance. Whereas, the number of multiple bounces

can be decreased in order to obtain low reflection loss performance by increasing the substrate thickness.

B. Design and Simulations

A thorough investigation has been carried out based on Finite Integral Method (FIM) using commercially available CST computer model to realize and demonstrate the effects of variable substrate thickness (0.508mm, 0.787mm, 1mm, 1.57mm, and 2mm) on the reflectivity performance of various reflectarray resonant elements. Three strategic resonant elements including dipole, square loop and triangular loop have been utilized to serve the purpose for operation in X-band (8-12GHz) frequency range. These reflectarray resonant elements under investigation are made to resonate at 10GHz in [19] for the characterization of reflection loss and reflection phase performance.

III. NUMERICAL MODEL

Realization of progressive phase distribution is an important parameter in reflectarray antenna design which is required to make a planar wave in front of the periodic aperture. Therefore, in this work a novel numerical model based on Periodic Method of Moment (MoM) has been derived to estimate the reflection phase values depicted by each individual resonant element. Material properties of the dielectric substrate, reflection area and surface current density of reflectarray resonant elements have been taken into consideration for an accurate implementation of the model as shown in (4):

$$\varphi = 2\pi \frac{\epsilon_r \tan \delta I_s}{W_g A_r t} \quad (4)$$

where φ is the desired reflection phase, 2π is the total phase range, ϵ_r is the relative permittivity, $\tan \delta$ is the loss tangent value, I_s is the surface current density, A_r is the area of resonant elements, t is the substrate thickness and W_g is the conditional arbitrary constant known as the guided wavelength factor whose range for the resonant elements mentioned in above section is given by (5) as:

$$0.02\lambda_g \leq W_g \leq 2.5\lambda_g \quad (5)$$

Whereas, the reflectarray antennas possess maximum reflectivity at the resonant frequency (f_r), hence the value of phase will be 0° at the point of maximum reflection. Remaining reflection phase values at ($f < f_r$) and ($f > f_r$) can be calculated by using (6):

$$\varphi = \begin{cases} 2\pi \frac{\epsilon_r \tan \delta I_s}{W_g A_r t} ; & f < f_r \\ 0 & ; f = f_r \\ -2\pi \frac{\epsilon_r \tan \delta I_s}{W_g A_r t} ; & f > f_r \end{cases} \quad (6)$$

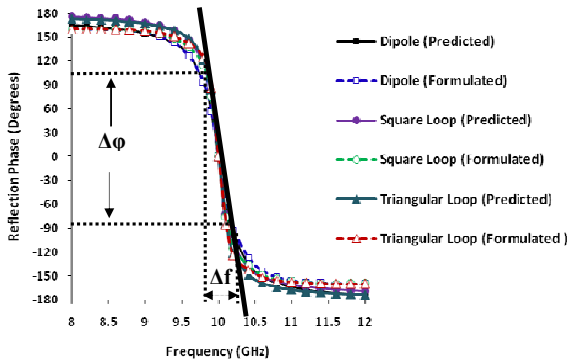


Fig. 2 Comparison of predicted and formulated reflection phase curves

The above equations can be used to find out the reflection phase values for reflectarray resonant elements with different substrate thicknesses by substituting the appropriate value of t . In order to validate the devised numerical model, a comparison between the predicted and formulated reflection phase curves of dipole, square loop and triangular loop has been presented in Fig. 2. It can be seen from Fig. 2 that the triangular loop element depicts the steepest reflection slope as compared to the dipole element which is shown to offer smoother reflection slope. Moreover, it can be seen that there exist a good agreement between the predicted and formulated reflection curves.

IV. FABRICATION AND MEASUREMENTS

A. Unit Cell Configurations

Two patch unit cells for each resonant element have been fabricated by utilizing two different substrate thicknesses of Rogers RT/Duroid 5870 dielectric material ($\epsilon_r=2.33$, $\tan\delta=0.0012$) in order to verify the theoretical results. The mutual coupling effects have also been taken into account by keeping the substrate dimensions constant for all the designed elements. Fig. 3 shows the fabricated samples of different strategic reflectarray resonant elements.

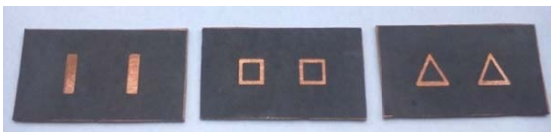


Fig. 3 Fabricated unit cell reflectarray resonant elements



Fig. 4 Dimension measurements for the approximation of fabrication errors



Fig. 5 Scattering parameters measurements setup

B. Dimensions Measurements

The digital vernier caliper is a precision instrument which can be used to measure the dimensions extremely accurately. Since the fabrication of the designed samples have been carried out manually using photolithography process, which may result in fabrication errors to due to random distribution of conductor patch (copper) on top of the dielectric substrate. Therefore the geometrical dimensions of the fabricated unit cell reflectarray resonant elements have been measured by using digital vernier caliper, in order to incorporate the fabrication errors as shown in the Fig. 4. The dimensions of the unit cell elements vary with the thickness of the dielectric substrate. There exist a minimum discrepancy of 0.07mm and maximum discrepancy of -0.48mm between the designed and measured dimensions. These fabrication errors will result in shifting of resonant frequency and higher reflection loss values of the reflectarray resonant elements.

C. Measurement Setup

The scattering parameter measurements of the fabricated two patch unit cell reflectarray resonant elements have been carried out using vector network analyzer as depicted in Fig. 5. The scattering behavior including reflection loss and reflection phase has been analyzed by connecting the standard X-Band waveguide simulator with the network analyzer via an Agilent coax to waveguide adaptor [20]. The two patch unit cell resonant elements are then inserted into 15mm \times 30mm aperture of the waveguide simulator as shown in Fig. 5. The ground plane of each element is taken as a reference and is subtracted from the measured values of reflection loss and reflection phase to get the actual curves of reflection loss and reflection phase response.

V. MEASURED RESULTS AND DISCUSSION

A. Reflection Loss Curves

Reflection loss is an important parameter for the performance characterization of reflectarrays. Generally the bandwidth performance of the reflectarray antennas can be analyzed by the reflection loss curve. In order to analyze the bandwidth performance, the bandwidth is defined by moving 10% above the maximum reflection loss value.

B. Reflection Phase Curves

Reflection phase is considered to be another crucial performance parameter used to analyze the reflectivity of reflectarrays. Moreover phase errors can also be observed

using reflection phase curves. The comparison of reflection phase performance can be indicated by Figure of Merit (FoM) and static phase range. FoM is defined in [21] as the change in the reflection phase to the change in frequency and can be expressed by using (7).

$$FoM = \frac{\Delta\varphi}{\Delta f} (\text{°/MHz}) \quad (7)$$

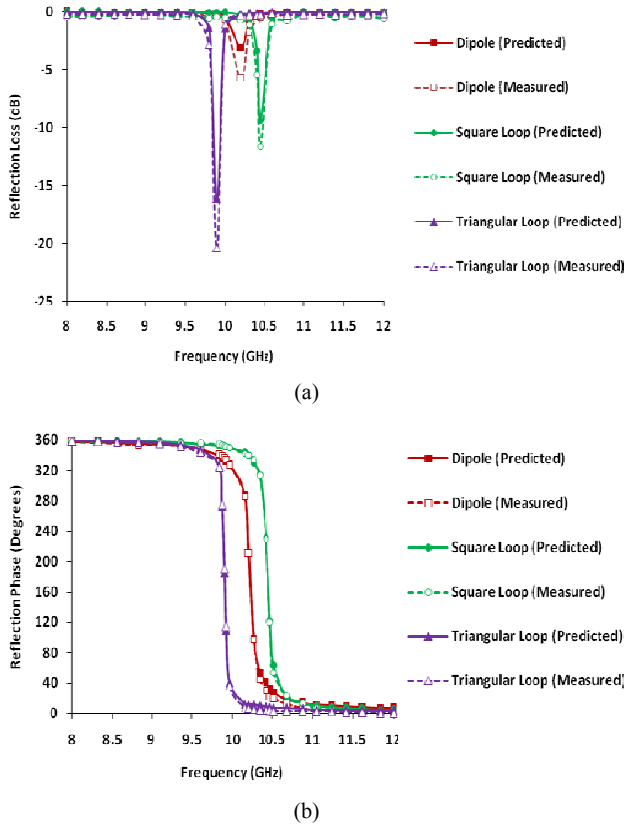


Fig. 6 Comparison of measured and predicted results for 0.508mm thick substrate (a) Reflection loss curves (b) Reflection phase curves

Fig. 6 shows the measured and predicted reflection loss and reflection phase curves for dipole, square loop and triangular loop element on 0.508mm thick substrate. In simulations all the resonant elements were made to resonate at 10GHz however; the resonant frequency of fabricated samples is shifted because of the fabrication errors as explained in section IV. It can be seen from Fig. 6 (a) that the maximum measured reflection loss of 20.25dB is depicted by the triangular loop element whereas, dipole element offer minimum measured reflection loss of 5.66dB. This is due to the fact that the thin substrate is utilized for the design of reflectarray resonant elements, and the dielectric absorption of incident electric fields cause rapid multiple bounces, thus offering higher reflection loss performance. Moreover it can be seen that the measured reflection loss is slightly higher than the predicted reflection loss. The losses in the waveguide simulator and connectors are the main reason for this discrepancy. As

depicted in Fig. 6 (b) the reflection phase slope of triangular loop element is steeper as compared to the dipole element which is shown to offer smooth reflection slope. Furthermore it can be observed that there exists a good agreement between the trend of both predicted and measured results.

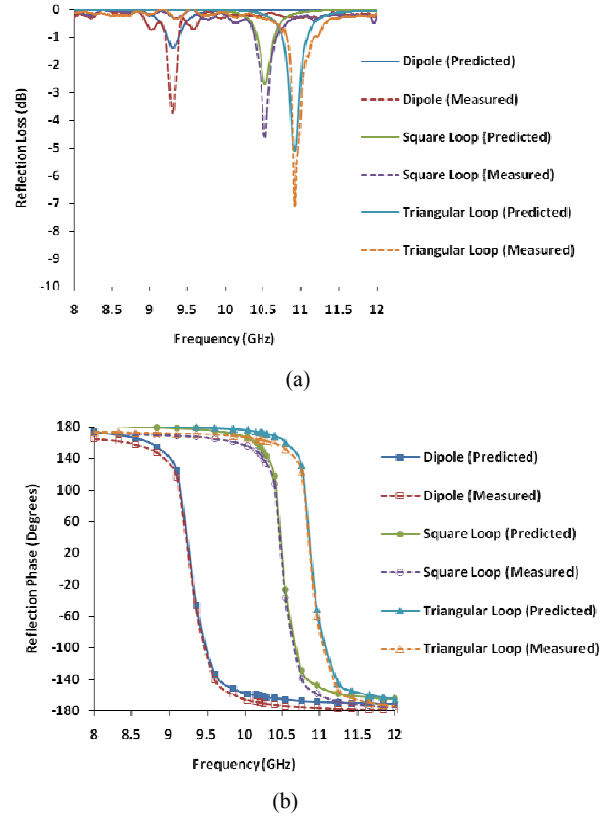


Fig. 7 Comparison of measured and predicted results for 0.787mm thick substrate (a) Reflection loss curves (b) Reflection phase curves

TABLE I
COMPARISON OF 10% BANDWIDTH, STATIC PHASE RANGE AND FOM

Resonant Elements	10% Bandwidth (MHz)		Static Phase Range (°)		Figure of Merit (FoM) (°/MHz)	
	0.508	0.787	0.508	0.787	0.508	0.787
	mm	mm	mm	mm	mm	mm
Dipole	39	64	260	250	0.97	0.93
Square Loop	27	48	270	260	1.03	0.97
Triangular Loop	12	23	290	280	1.16	1.12

The measured reflection loss and reflection phase curves for all the resonant elements on 0.787mm thick substrate are presented in Fig. 7. It can be seen from Figs. 6 and 7 that as the substrate thickness is increased from 0.508mm to 0.787mm the measured reflection loss value of triangular loop element decreased from 20.5dB to 7.02dB and measured reflection loss value of dipole element decreased from 5.66dB to 3.70dB. Moreover it is demonstrated in Fig. 7 (b) that with an increase in the substrate thickness the reflection phase curves for all the resonant elements change their trend from steep slope to significantly smoother slope.

C. Bandwidth, Static Phase Range and Figure of Merit (FoM)

Table I summarizes the measured 10% bandwidth, static phase range and FoM values of all the resonant elements under investigation. From Table I, it can be observed that dipole element with the minimum FoM value of 0.97°/MHz and 0.93°/MHz offers a minimum static phase range of 260° and 250° with maximum 10% bandwidth of 64MHz and 39MHz whereas, triangular loop with maximum FoM value of 1.16°/MHz and 1.12 °/MHz is shown to give maximum static phase range of 290° and 280° with minimum 10% bandwidth of 23MHz and 12MHz. Therefore it can be concluded that as the substrate thickness increases the 10% bandwidth increases whereas, static phase range and FoM decreases.

VI. CONCLUSION

Dielectric absorption in the substrate region of reflectarrays has been exploited by mounting various strategic reflectarray resonant elements on variable substrate thicknesses. It has been demonstrated that the dielectric materials plays an effective role in enhancing the reflectivity performance of reflectarrays. Moreover a numerical model has been established to realize the progressive phase distribution of reflectarray resonant elements. Two patch unit cell reflectarray have also been fabricated to carry out the waveguide simulator technique for the performance realization of each thickness separately. It can be observed that the reflection loss decreases with an increase in the substrate thickness. The dipole element is shown to offer the minimum measured reflection loss of 3.70dB with the highest 10% bandwidth performance of 64MHz. Whereas, the triangular loop element depicts the maximum measured loss of 20.25dB with the highest static phase range performance of 290°. Therefore it can be concluded that by employing thick substrate the feasibility to enhance the bandwidth performance can be realized. However the increase in the bandwidth performance has to be traded-off with the static phase range performance of the reflectarrays.

ACKNOWLEDGMENT

This research work is fully funded by the Prototype Research Grant Scheme (PRGS VOT 0904) awarded by the Ministry of Higher Education (MOHE), Malaysia. The authors would like to thank the staff of Wireless and Radio Science Centre (WARAS) for the technical support.

REFERENCES

- [1] G. D. G. Berry, R.G. Malech and W. A. Kennedy, "The Reflectarray Antenna", IEEE Trans. on Antennas and Propagat., Vol. AP11, Nov 1963.
- [2] J. Huang and J. Encinar, "Reflectarray Antennas", Wiley, Interscience, 2007.
- [3] J. Huang, "Analysis of a Microstrip Reflectarray Antenna for Microspacecraft Applications", TDA Progress Report 42-120, 1995.
- [4] D. M. Pozar and S. D. Targonski, H. D. Syrigos, "Design of Millimeter Wave Microstrip Reflectarrays", IEEE Tran. on Antennas and Propagat., Vol 45, No. 2, pp. 287-296, 1997.
- [5] R. D. Javor, X. D. Wu and K. Chang, "Design and Performance of Microstrip Reflectarray Antenna," IEEE Transactions on Antennas and Propagation, Vol. 43, No. 9, pp. 932-938, 1995.
- [6] N. F. Kiyani and M. Hajian, "Design, Analysis and Measurements of Reflectarray Using Variable Length Microstrip Patch Antennas at Ka-Band," The 18th Annual IEEE International Symposium on Personal, Indoor and Mobile Radio Communication, pp. 1-5, 2007.
- [7] S. D. Targonski and D. M. Pozar, "Analysis and Design of a Microstrip Reflectarray Using Patches of Variable Size," IEEE Antennas and Propagation Society International Symposium, Vol. 3, pp. 1820-1823, 1994.
- [8] J. Huang and R. J. Pogorzelski, "Microstrip Reflectarray with Elements Having Variable Rotation Angle," IEEE Antennas and Propagation Society International Symposium, Vol. 2, pp. 1280-1283, 1993.
- [9] M. E. Bialkowski, A.M. Abbosh and K. H. Sayidmarie "Investigations into Phasing Characteristics of Printed Single and Double Cross Elements for Use in a Single Layer Microstrip Reflectarray," IEEE Antennas and Propagation Society International Symposium, 2008.
- [10] D. M. Pozar and S. D. Targonski, "A Microstrip Reflectarray Using Crossed Dipoles," IEEE Antennas and Propagation Society International Symposium, Vol. 2, pp. 1008-1011, 1998.
- [11] N. Misran, R. Cahill and V.F. Fusco, "Reflection Phase Response of Microstrip Stacked Ring Elements", Electronics Letters, Vol. 38, No.8, pp. 356-357, 2002.
- [12] K. H. Sayidmarie and M. E. Bialkowski, "Multi-Ring Unit Cells for Increased Phasing Range in Single Layer Microstrip Reflectarrays," Proceedings of iWAT, pp. 163-166, 2008.
- [13] W. Hu, M. Y. Ismail, R. Cahil, J. A. Encinar, V. F. Fusco, H. S. Gamble, D. Linton, R. Dickie, N. Grant, and S. P. Rea, "Liquid-Crystal-Based Reflectarray Antenna with Electronically Switchable Monopulse Patterns", Electronics Letters, Vol. 43, No. 14, 2007.
- [14] M. Y. Ismail and M. Inam, "Analysis of Design Optimization of Bandwidth and Loss Performance of Reflectarray Antennas Based On Material Properties", Modern Applied Sci. J. CCSE., Vol. 4, No.1, pp. 28-35, 2010.
- [15] D. M. Pozar and S. D. Targonski, "A Shaped-Beam Microstrip Patch Reflectarray", IEEE Trans. on Antennas and Propagat., Vol. 47, No. 7, February 1999.
- [16] K. Y. SZE and L. Shafal, "Analysis of Phase Variation Due to Varying Patch Length in a Microstrip Reflectarray", IEEE Trans. on Antennas and Propagat., Vol. 46, No. 7, pp. 1134-1137.
- [17] J. A. Encinar, M. Arrebola, M. Dejus and C. Jouve, "Design of a 1-Meter Reflectarray for DBS Application with 15% Bandwidth", 1st European Conference on Antennas and Propagation, pp. 1-5, 2006.
- [18] M. Y. Ismail, M. Inam and A. M. A. Zain, "Reflectivity of Reflectarrays Based On Dielectric Substrates", American Journal of Engineering and Applied Sciences, pp. 180-185, 2010.
- [19] Arslan Kiyani and M. Y. Ismail, "Design and Analysis of High Performance Reflectarray Resonant Elements", Procedia Engineering, Vol. 53, pp. 248-254, 2013.
- [20] M. Y. Ismail and Arslan Kiyani, "Investigation of Reflection Area on Strategic Reflectarray Resonant Elements", International Symposium on Wireless Technology and Applications (ISWTA), pp. 363-367, 2013.
- [21] M. Y. Ismail and M. Inam, "Resonant Elements for Tunable Reflectarray Antenna Design", International Journal of Antennas and Propagation, Vol. 2012, pp. 1-6, 2012.